Journal of Physics:
Conference Series

PURPOSE-LED PUBLISHING™

PAPER • **OPEN ACCESS**

Structural, Optical, and Electrical Transformations in $Fe_xSi_{1-x}O$ Thin Films: The Role of Iron and Annealing

To cite this article: M Sudha *et al* 2024 *J. Phys.: Conf. Ser.* **2837** 012020

View the article online for updates and enhancements.

You may also like

- Design and Analysis of CVT Cooling System
C. Parswajinan, S. Rajesh, B. Vijaya Ramnath et al.
- Advanced Machining Performance Through Optimization of Awjm Parameters using Metaheuristic Techniques
P Jai Rajesh, V. Balambica and M. Achudhan
- Flexural and Shear Strength Analysis of Kevlar/Carbon-Epoxy Composites using Finite Element Modelling
M Mohammed Mohaideen, Bandi Sriya, Kolakani Anusha et al.

This content was downloaded from IP address 103.196.31.194 on 19/12/2024 at 07:56

Journal of Physics: Conference Series **2837** (2024) 012020 doi:10.1088/1742-6596/2837/1/012020

Structural, Optical, and Electrical Transformations in $Fe_xSi_{1-x}O$ Thin Films: The Role of Iron and Annealing

Sudha M[1], Balamurugan A[2], Girisha L[3], Kalaiarasan S[4], Ravivarman G[5], Nanthakumar S[6], Girimurugan R[7*]

[1]Assistant Professor, Department of Physics, Government Arts College, Udhagamandalam 643 002, Tamilnadu, India

[2]Assistant Professor, Department of Physics, Government Arts and Science College, Avinashi 641 654, Tamilnadu, India

[3]Professor, Department of Mechanical Engineering, PES Institute of Technology and Management, Shivamogga 577 204, Karnataka, India

[4]Assistant Professor, Department of Chemistry, Sona College of Technology, Salem 636 005, Tamilnadu, India"

[5]Assistant Professor, Department of Electrical and Electronics Engineering, Karpagam Academy of Higher Education, Coimbatore 641 021, Tamilnadu, India.

[6]Assistant Professor (Senior Grade), Department of Mechanical Engineering, PSG Institute of Technology and Applied Research, Coimbatore 641 062, Tamilnadu, India

[7]Assistant Professor, Department of Mechanical Engineering, Nandha College of Technology, Perundurai 638 052, Tamilnadu, India

[*]Corresponding author: dr.r.girimurugan@gmail.com

Abstract. Thin films $Fe_xSi_{1-x}O$, with iron (Fe) content between 0 to 20% have been applied to substrates made of soda lime glass by means of the spray pyrolysis process. Annealing the films allowed us to test their thermal stability. Both the as-deposited$Fe_xSi_{1-x}O$ thin film and annealed Fe_xSi_{1-x}Othin film were analyzed by. Researchers analyzed the structure of the films and its composition using these methods. The XRD study demonstrated that the Fe_xSi_{1-x}Othin films, even if they are deposited or annealed, have a wurtzite structure in the plane orientation. The result shows that the films' crystalline structure is not affected by the heating process. In addition to that, the good indicator of film quality and consistency were no signs of pinholes or cracks in the films. An iron deficiency was identified by following the annealing process, according to the compositional analysis done by EDAX. Annealing affects the integration of Fe in the film's matrix, according to these changes occur in the composition. The band gap changes to red for Fe_xSi_{1-x}Othin films was observed in the optical characteristics of these films while tested using Ultra Violet -Visible spectroscopy. Integrating Fe into films alters their electronic structure, and it is one important indicator for band gap change. The incorporation of Fe resulted in a reduction in resistance and it is measured by the electrical properties using the two-probe method which in turn indicates an improvement in the films' electrical conductivity. In conclusion, the outcomes if this research supports the feasibility of incorporating iron into the silicon carbide thin films. There are major structural changes to the films' electrical characteristics and optical properties due to this incorporation.

Content from this work may be used under the terms of the Creative Commons Attribution 4.0 licence. Any further distribution of this work must maintain attribution to the author(s) and the title of the work, journal citation and DOI.
Published under licence by IOP Publishing Ltd

The outcomes of this research have significant implications for the advancement of electronic and optoelectronic devices that could make use of these alterations to enhance their performance.

Keywords: $Fe_xSi_{1-x}O$, spray pyrolysis technique, thin films, electrical conductivity, band gap.

1. Introduction

The potential to create materials with different topological structures has piqued the interest of many researchers in silicon carbide (SiC). These structures impact optical properties and density of electronic states. The structural versatility, electronic behavior, and photo luminescent response of this material go well beyond its mechanical hardness and good thermal stability [1-2]. Thin film LED's, electroluminescent devices, and heterojunction bipolar transistors are just a few of the optoelectronic and microelectronic applications that have garnered a lot of attention for SiC, whether it's amorphous or crystalline [3-4]. Crystalline SiC shows promise as an electronic device material. High frequency and temperature and high power appliances can benefit from its basic characteristics that comprise a wide band gap, a high saturation drift velocity and thermal conductivity and a strong electrical breakdown field [5-6]. Concurrently, SiC developed the combination of Si's electronic and micromachining capabilities with Si's high temperature capabilities. Nevertheless, current begins to flow through the Si substrate as a consequence of the SiC/Si heterojunction leaking at temperatures greater than 500 K [7-8]. Creating SiC-on-insulator (SiCOI) structures by depositing SiC onto SOI (silicon on insulator) substrates is one way to sidestep this issue. In addition to their usefulness as large-area, low-cost substrates for optoelectronic and high-temperature applications, these structures are also attractive for use in micromechanical devices that operate in physically or chemically hostile environments, as well as in high-frequency, high-power smart-sensors [9-10]. The fabrication of high-quality SiC thin films has been accompanied through the use of a variety of growth methods. The known plasma-enhanced chemical vapor deposition (PECVD) is a flexible and tried-and-true method [11-12]. By adjusting technical parameters, this method opens the door to low-temperature structure design and the modification of microstructure-related properties in films. Additionally, it makes it possible for large-area films to grow [13]. Numerous advantages to human life have resulted from the exploration of compound semiconductor materials with wide band gaps. The use of materials such as Al xGa1−xN, BN, and SiC in devices such as UV-LEDs, lasers, and thin-film transistors piqued interests. An important material with many uses, including solar cells is silicon carbide (SiC), which is abundant on Earth and has a wide band gap [14], [15]. Owing to its high excit on binding energy of 60 meV—that can be enhanced to 100 meV in super lattices—it is assuring material for LEDs and lasers [16]. One possible use for SiC is to create Electro Magnetic Interference shielding coatings or heat/microwave reflecting window coatings, as it reflects thermal infrared heat [17-18]. Changing the optical and electrical characteristics of SiC is a crucial step in developing opto-electronic devices based on this material. Dopants such as In, Ga, Al etc., enhances the high n-type conductivity of SiC, a known n-type semiconductor material. Another way to make p-type SiC is to dope it with elements like Bi, As, P, etc. As an example, alloying SiC with Mg can increase its optical band gap to 4.5 eV. It is also possible to engineer a lower band gap using Fe [19-20]. The crystal structures of hexagonal SiC and cubic Fe_2O_3 are extremely different. Additionally, grown single-phase hexagonal $Fe_xSi_{1-x}O$thin films with a high Fe concentration are extremely challenging due to the low thermodynamic solubility of Fe_2O_3 (~ 2 mol. %) in Fe_2O_3-SiC systems [21-22]. Spray pyrolysis, Molecular beam epitaxy, sputtering and deposition of pulsed laser are some of the techniques that can be employed to grow mixed $Fe_xSi_{1-x}O$thin films. As far as industrially applicable methods for creating thin films of metal oxides, spray pyrolysis is the simplest method. The spray pyrolysis methodology allows for the rapid growth of thin films over enormous areas. Few studies have utilized the spray pyrolysis technique is used to fabricate thin films of [$Fe_xSi_{1-x}O$ ($0 \leq x \leq 0.20$)]. So, this study is all about the effects of heating on the characteristics of $Fe_xSi_{1-x}O$thin films that were deposited using the spray pyrolysis technique. In addition, the purity of phase, surface

morphology characteristics, optical characteristics and electrical characteristics, and annealed and as-deposited $Fe_xSi_{1-x}O$ thin films are examined.

2. Experimentation

As demonstrated, the well-cleaned soda lime glass is covered with thin films of $Fe_xSi_{1-x}O$using the spray pyrolysis technique. Thin films of $Fe_xSi_{1-x}O$ (where x is an integer from 0 to 0.20) are produced by dissolving the precursor materials like Silicon diacetate dihydrate (Si $(CH_3COO)_2 \cdot 2H_2O$) and iron chloride ($FeCl_2 \cdot 2^{1/2}H_2O$) in distilled water in varying molar ratios. A spray nozzle was used to atomize the precursor solution, which was then sprayed onto a glass substrate that is preheated at an optimized temperature of approximately 400 °C at a rate of 2 ml/min. Atmosphere is utilized as the carrier gas at a 2 bar pressure, and the space between the glass substrate and spray nozzle is fixed at 30 cm. Thin films of highly adherent $Fe_xSi_{1-x}O$are formed when the heated glass substrate is reached by the atomized droplets, which oxidize on it. Figure. 1 shows the schematic view of Spray pyrolysis setup.

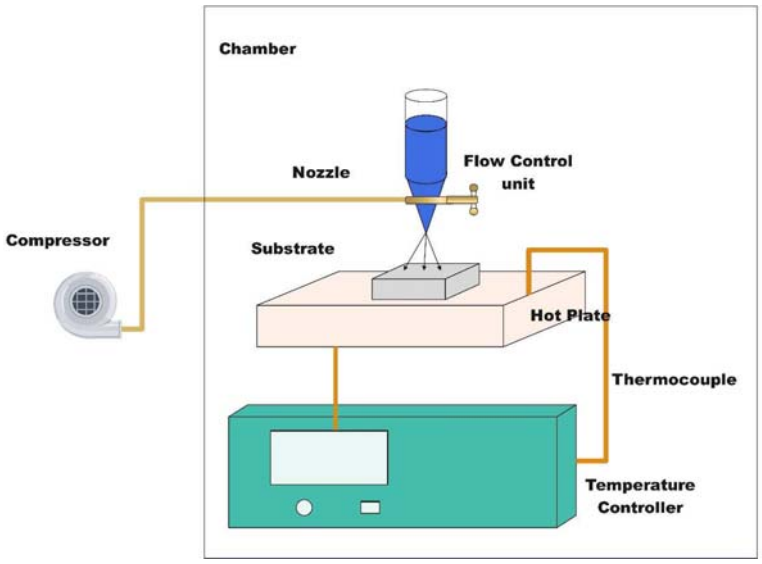

Figure 1. Schematic view of spray pyrolysis setup

The gravimetric technique is used to measure the thin film thickness, which is kept at approximately 600 nm. The X-ray diffractometer is used to examine the thin film's crystallinity and its phase made by $Fe_xSi_{1-x}O$. The chemical composition and surface morphology of the grown film are examined. A UV-V spectrophotometer is utilized to assess the optical transmittance of thin films made of $Fe_xSi_{1-x}O$. A computer-interfaced Keithley source metre is used to conduct the electrical measurements. A computer-interfaced Keithley source metre is used to conduct the electrical measurements.

3. Results and Discussions

3.1 XRD

The nature of the produced$Fe_xSi_{1-x}O$thin films is revealed to be polycrystalline by the XRD studies. The structure in the hexagonal wurtzite shape, oriented along the c-axis, is seen in the films. If the peak along the plane is sharper, it means the thin film has good crystallinity. The fact that there is no visible peak for Fe_2O_3 indicates that the iron has been evenly distributed

throughout the thin film and has not precipitated out as an impurity phase. The peak positions of $Fe_xSi_{1-x}O$ thin films, considering the function of Fe content, are given in Table 1.

Table 1. $Fe_xSi_{1-x}O$ structural parameters determined by X-ray Diffraction

Name of the Specimen	As-deposited Specimen			Annealed Specimen		
	D (nm)	2*θ* (°)	*d* (Å)	*D* (nm)	2*θ* (°)	*d* (Å)
SiC	30	39.46	4.028	32	39.45	4.028
Fe0.06Si0.94 C	32	39.43	4.03	34	39.44	4.029
Fe0.12Si0.88 C	33	39.36	4.038	40	39.4	4.036
Fe0.24Si0.76 C	32	39.3	4.039	33	39.33	4.037

The fact that the peak moves downwards slightly when Fe is added indicates that Fe^{2+} atoms have replaced Si^{2+}. According to Bragg's equation, the inter planar distance denoted by d is recorded in the tabulation [23].

$$2dhkl\ sin\theta = n\lambda \tag{1}$$

Where, n denotes the diffraction order and hkl denotes the Miller indices of the diffraction plane. To determine the cell volume that is represented by *v* and the lattice factors described as 'a' and 'c' for a structure in hexagonal shape [24-26].

$$v = \frac{\sqrt{3}}{2}a^2c \tag{2}$$

$$\frac{1}{d^2} = \frac{4}{3}\frac{(h^2+hk+k^2)}{a^2} + \frac{l^2}{c^2} \tag{3}$$

Figure. 2 shows a plot of the evaluated cell volume v and the lattice parameters described by a and c by using the X-ray Diffraction data as a function of concentration of iron. Interplanar distance d, cell volume v, lattice parameters that is a and c, and iron content all show a small increase with increasing iron content. The crystal undergoes a transformation due to the fact that the cationic radii of Fe^{2+} (0.97 Å) and Zn^{2+} (0.74 Å) are distinct. According to Table 1, which displays the computed average grain size, with the rises in Fe concentration, the average grain size also increases.

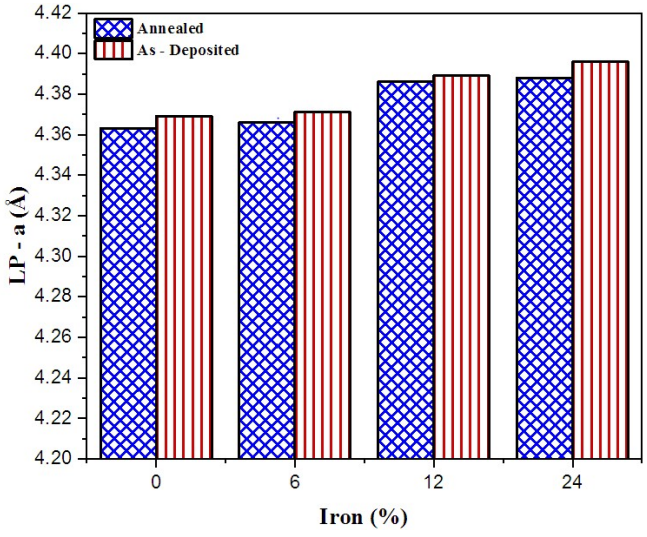

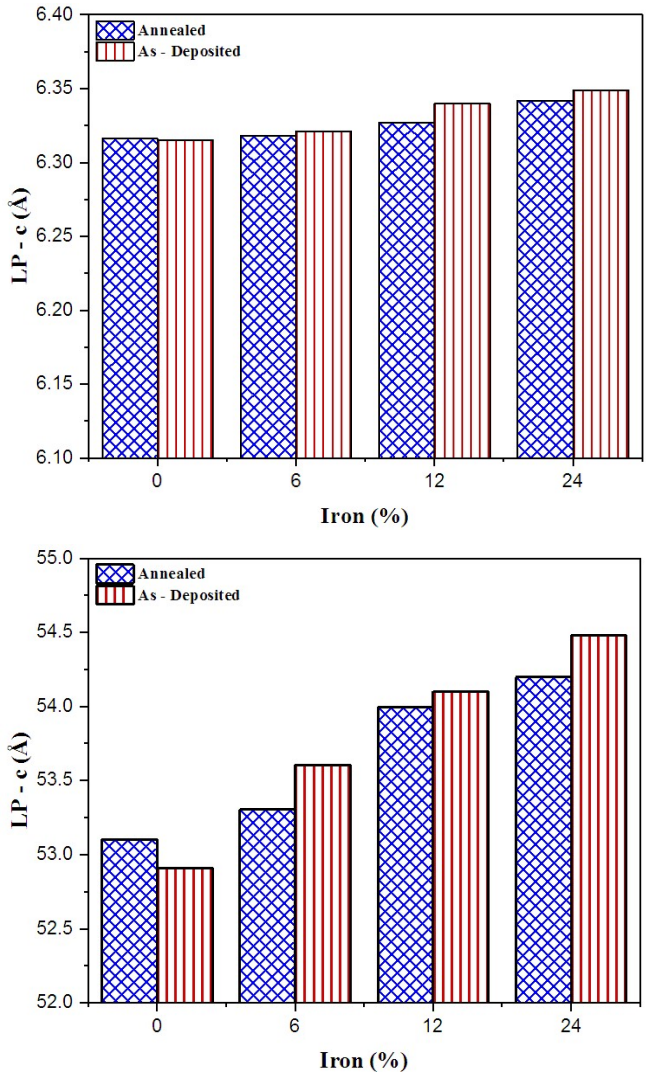

Figure 2. Iron content dependence of Lattice parameters a, b, and c as well as cell volume c

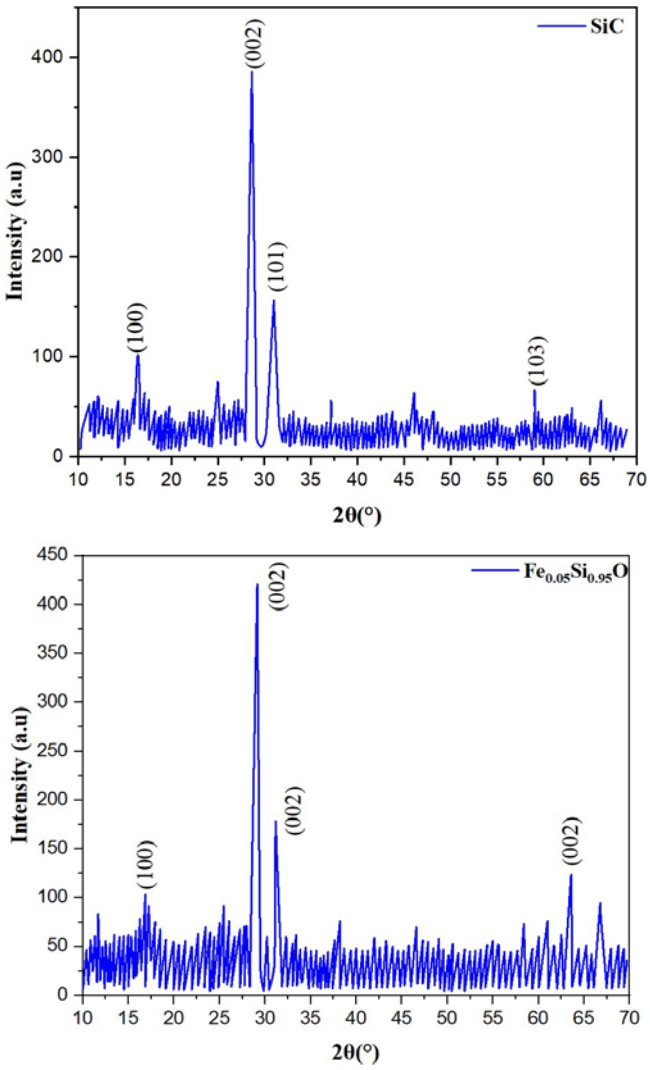
SiC
(002)
(101)
(100)
(103)
Intensity (a.u)
2θ(°)
Fe0.05Si0.95O
(002)
(002)
(100)
(002)
Intensity (a.u)
2θ(°)

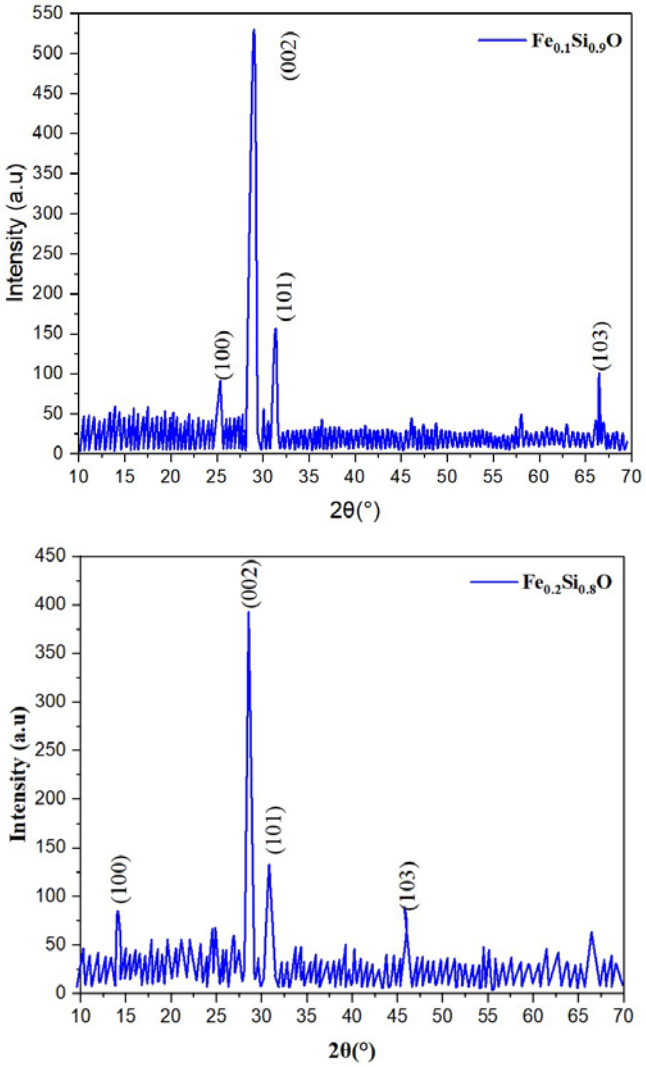

Figure 3. Annealed thin films of $Fe_xSi_{1-x}O$ with XRD spectra at (a) 0 %, (b) 6 %, (c) 12%, and (d) 24 %

Additionally, all of the thin films that get deposited are heated by air for 4 hours at 400 °C to ensure thermal stability. Annealed thin films with various Fe concentrations are indicates in the XRD spectra in Figure. 3. According to the patterns of X Ray Diffraction, the annealed or heated films also have a polycrystalline hexagonal crystal-like structure [27-28]. Also, annealing has no impact on the preferred orientation of the $Fe_xSi_{1-x}O$ thin films that are deposited. Table 1 shows that compared to as-deposited thin films, annealed$Fe_xSi_{1-x}O$ thin films have a smaller move in the peak position of the plane. The lattice factors that is a and c and the cell volume v, of the heated thin films are smaller when contrasted to the as-deposited $Fe_xSi_{1-x}O$ thin films, as shown in Figure 3. This could be because the annealing process causes some of the Fe to evaporate back into the material, lowering its concentration. The recrystallization process that occurs during annealing may be the reason why grain size increases after annealing for all compositions of $Fe_xSi_{1-x}O$ thin films.

3.2 Basic analysis

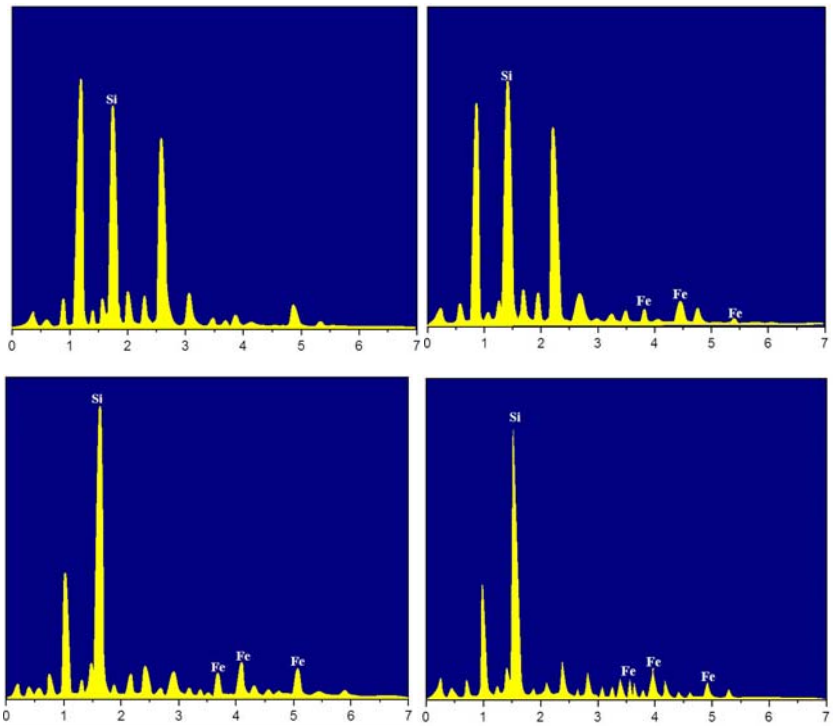

Figure 4. The EDAX spectra of annealed $Fe_xSi_{1-x}O$ thin films were measured for various iron concentrations, with a setting at (a) 0%, (b) 6%, (c) 12%, and (d) 24%.

Figure. 4 displays the spectrum of EDAX obtained from the compositional studies of the prepared $Fe_xSi_{1-x}O$ thin films that were conducted using EDX. The EDX spectra provide conclusive evidence of oxygen, Fe, and Si. Also visible are impurities originating from the glass substrate, such as sodium and silicon. The prepared $Fe_xSi_{1-x}O$thin film has a lower amount of Fe than the starting solution, it is clear. The data regarding the composition of the thin films as they were deposited are presented in Table 2. Because Fe evaporates during annealing, the atomic concentration of Fe drops even lower after the process. Results from XRD analysis corroborate these findings.

Table 2 $Fe_xSi_{1-x}O$ thin films atomic percentage of Fe and Si

Name of the Specimens	As-deposited Specimens		Annealed Specimens	
	Si (at. %)	Fe (at. %)	Si (at. %)	Fe (at. %)
SiC	100	0	100	0
Fe 0.06Si0.94 C	96.25	3.75	98.5	1.5
Fe 0.12Si0.88 C	94.6	5.4	95.78	4.22
Fe 0.24Si0.76 C	89.78	10.22	90.25	9.75

3.3 Optical Characteristics

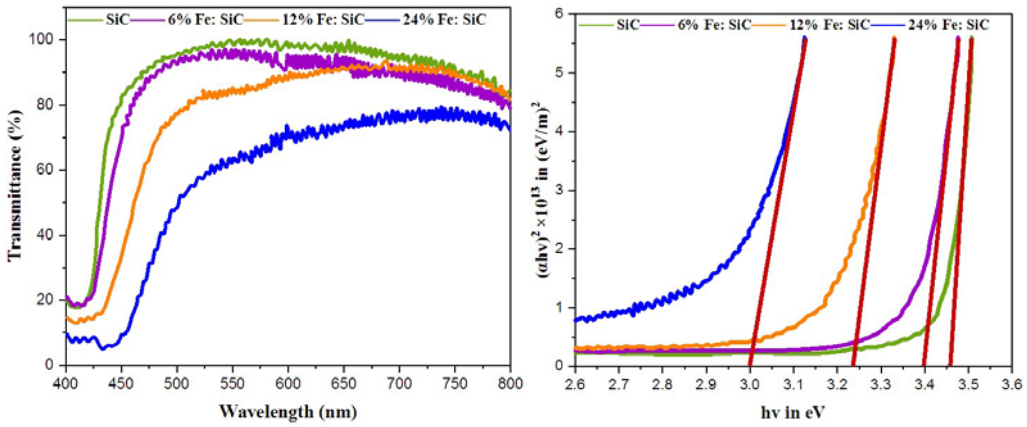

Figure 5. (a) Spectra of Transmittance, (b) annealed $Fe_xSi_{1-x}O$ thin films' Tauc's plots

Figure. 5 (a) displays the optical transmittance at normal temperature for all as-received$Fe_xSi_{1-x}O$ thin films. With a transmittance of greater than 95%, the pure as-deposited SiC samples are extremely see-through in the visible light spectrum. At 24 %, the transmittance value drops to approximately 60 % as the Fe concentration rises. Increased surface roughness, which scatters light, and increased free electron absorption, which is compatible with decreased resistivity, is two possible explanations for the drop in transmittance [29-30]. The range of the band gap are identified by plotting $(\alpha hv)^2$ against (hν). Extrapolating the linear portion of $(\alpha hv)^2$ axis to the (hν) axis determines the band gap value. The value of band gap is appeared to be reduced with increasing Fe. It is possible to see the evaluated band gap values in Table 3. The replacement of Fe^{2+} ions for Zn^{2+} ions in the SiC lattice causes the band gap values to lessen. The band gap increases slightly after annealing, but the transmittance value stays nearly the same. Based on the results of the XRD and EDX analyses, the small increment in band gap might be due to the Fe evaporation from the SiC lattice.

Table 3. Band gap of thin films of $Fe_xSi_{1-x}O$, both as-deposited and after annealing

Specimens Name	As-deposited $Fe_xSi_{1-x}O$ (eV)	Annealed $Fe_xSi_{1-x}O$ (eV)
SiC	4.48	4.51
Fe 0.06Si0.94 C	4.43	4.44
Fe 0.12Si0.88 C	4.21	4.31
Fe 0.24Si0.76 C	4.04	4.08

3.4 Electrical characteristics

The hot-probe experiment confirmed that all of the as-received thin films exhibited conductivity that is n-type. The thin film's linear ohmic nature is revealed by the 1 to 5analysis of thin films containing co-planar contacts made of aluminium. Table 4 displays the calculated conductivity and measured resistance of the $Fe_xSi_{1-x}O$ thin film. A thin film of $Fe_xSi_{1-x}O$ has an increased conductivity up to 12% as the concentration of Fe increases. There is an increase in conductivity because the iron atom, which may be located in the interstitial position of the SiC lattice, donates two electrons to the conduction band. The conductivity drops at 24 at. percent Fe, which XRD measurements suggest may be due to a reduction in crystallinity. The conductivity of all the $Fe_xSi_{1-x}O$ thin films is found to decrease following annealing. According to the results of the EDX analysis, the conductivity drops because iron evaporates. Figure 6. shows the I to V characteristic graphical curve for as-deposited SiC thin film and Fe 0.05Si0.95O thin film.

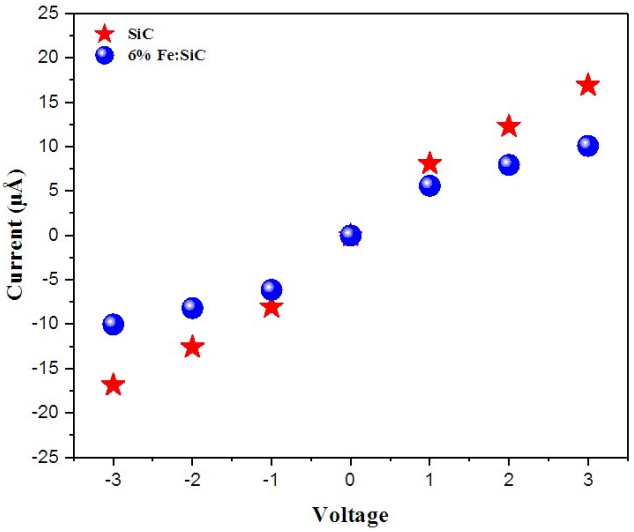

Figure 6. I to V characteristic graphical curve for as-deposited SiC thin film and Fe 0.05Si0.95O thin film

Table 4. Electrical data for as-deposited $Fe_xSi_{1-x}O$ thin film and annealed $Fe_xSi_{1-x}O$ thin film

Name of the Specimens	As-deposited specimen		Annealed specimen	
	Resistance (Ω)	Conductivity (S/m)	Resistance (Ω)	Conductivity (S/m)
SiC	4.1 MΩ	0.1	11.9 MΩ	0.021
Fe 0.05Si0.95 C	41 kΩ	5.07	3.6 MΩ	0.078
Fe 0.1Si0.9 C	5.19 kΩ	43.62	185 kΩ	0.947
Fe 0.2Si0.8 C	48 kΩ	4.42	235 kΩ	0.812

4. Conclusions

Soda lime glass substrates have been effectively coated with thin films of $Fe_xSi_{1-x}O$, where the iron (Fe) content ranges from 0 to 0.20. A wurtzite crystal structure, mainly aligned along the direction, is visible in these films. Evidence of Fe incorporation into the SiC lattice is clearly shown by a noticeable shift in the peak position in the crystal structure. Adding Fe does not alter the thin films' desired orientation in any way, even after annealing. Nevertheless, the film's properties undergo a small change during annealing, which includes a decrease in the Fe content. Varying the Fe concentration also affects the optical characteristics of the films. As the percentage of iron rises, the band gap values move to the red end of the spectrum. According to the band gap shift, the incorporation of Fe has altered the electrical properties. Another interesting aspect of this study is the results regarding the electrical conductivity of the SiC thin films. The initial conductivity is very high at the deposited SiC films. This conductivity increases gradually by the addition of iron. In accordance with this enhancement, Fe is the significant material that alters the electrical characteristics in the SiC films. These materials could be utilized variously in electronic and optoelectronic applications that controlled regulated conductivity, depending on the outcome of this realization. Considerate the impact of metal integration on the electric properties and structural features of semiconductor thin films has been greatly enhanced by this study.

References

[1] Irani R, Rozati S M and Beke S 2018 *Applied Physics A*. **124** 1.
[2] Suryawanshi D N, Pathan I G, Bari A and Patil L.A 2018 *AIP Conference Proceedings.* **1953.**
[3] Belkhalfa H, Ayed H, Hafdallah A, Aida M S and Ighil R T 2016 *Optik.* **127** 2336
[4] Babu B, Meinathan S, Manikandan P, Lingeswaran P, Nanthakumar S, Yasminebegum A and Girimurugan R 2023 *Journal of Physics: Conference Series.* **2603** 012041
[5] Aboud A A, Mukherjee A, Revaprasadu N and Mohamed A N 2019 *Journal of Materials Research and Technology*. **8** 2021
[6] Beji N, Souli M, Azzaza S, Alleg S and Kamoun Turki N 2016 *Journal of Materials Science: Materials in Electronics.* **27** 4849
[7] Illakkiya J T, Rajalakshmi P U and Oommen R 2015 *Int J Chemtech Res*. **7** 1032
[8] Ponnusamy P, Girisha L, Balamurugan S, Benham A, Vivek R, Loganathan G B and Girimurugan R 2023 *Journal of Physics: Conference Series*. **2603** 012038
[9] Hanna Scarlet R S, Sriram S and Balamurugan D 2016 *Asian Journal of Applied Sciences.* **9** 13
[10] Manogowri R, Mary Mathelane R, Valanarasu S, Kulandaisamy I, Benazir Fathima A and Kathalingam A 2016 *Journal of Materials Science: Materials in Electronics*. **27** 3860
[11] Aoun Y, Benhaoua B, Gasmi B and Benramache S 2015 *Main Group Chemistry*. **14** 27
[12] Hadri A, Taibi M and Mzerd A 2016 *Journal of Physics: Conference Series.* **689** 012024
[13] Yeşilkaya S S and Ulutaş U 2020 *Research on Engineering Structures and Materials*. **6** 119
[14] Thahab S M, Alkhayatt A H O and Zgair I A 2016 *Mater Sci Semicond Process*. **41** 436
[15] Girimurugan R, Senniangiri N, Krishnan B P, Kavitha S and Vairavel M 2021 *IOP Conference Series: Materials Science and Engineering* **1059** 012033
[16] Aoun Y, Benhaoua B, Benramache S Gasmi B 2015 *Optik (Stuttg).* **126** 5407
[17] Pandeeswari R and Jeyaprakash B G 2016 *Adv Sci Lett*. **22** 730
[18] Kennedy A, Viswanathan K, Krishnamoorthy N and Pradeev Raj K 2016 Mater Sci Semicond Process. **48** 39
[19] Yelsani V, Pothukanuri N, Sontu U B, Yaragani V and. Musku Venkata R R 2019 *Medziagotyra.* **25** 3
[20] Balamurugan S, Rajalakshmi A and Balamurugan D 2015 *J Alloys Compd*. **650** 863
[21] Beji N, Souli M, Reghima M, Azzaza S, Safia A and Kamoun-Turki N 2017 *J Electron Mater.* **46** 6628
[22] Jayaraman R, Girimurugan R, Suresh V, Shilaja C and Mayakannan S, 2022 *ECS Transactions*. **107** 7265
[23] Adeoye Victor B 2017 *NuclInstrum Methods Phys Res B*. **413** 57
[24] Beji N, Souli M, Reghima M, Azzaza S, Alleg S and Kamoun-Turki N 2016 *Mater Sci Semicond Process*. **56** 20
[25] Kim C and Hong S 2017 *Molecular Crystals and Liquid Crystals*. **645** 217
[26] Subha K, Ravichandran K and Sriram S 2017 *Appl Surf Sci*. **409** 413
[27] Girimurugan R, Vairavel M, Shanjai S D, Manikandan S, Manikkumar R and Manojkumar R 2020 *International Journal of Innovative Technology and Exploring Engineering*. **9** 2279
[28] Bchiri Y, Bouguila N, Kraini M and Alaya S 2019 *Surface Review and Letters*. **26** 1850223
[29] Dineshbabu N and Ravichandran K 2017 *Mater Res Express*. **4** 096410
[30] Noorunisha T, Nagarethinam V S, Suganya M, Praba D, Ilangovan S, Usharani K and Balu A R 2016 *Optik.* **127** 2822